STRUCTURAL PERFORMANCE OF SIDE COLUMNS SUBJECTED TO VARYING AXIAL LOAD

N. Teramoto[1] ,T. Nishida[2] and J. Kobayashi[3]

[1] *Assistant Professor, Dept. of Architecture & Environment System, Akita Prefectural University, Akita, Japan*
[2] *Associate Professor, Dept. of Architecture & Environment System, Akita Prefectural University, Akita, Japan*
[3] *Professor, Dept. of Architecture & Environment System, Akita Prefectural University, Akita, Japan*
Email: tera@akita-pu.ac.jp, tetsuya_nishida@akita-pu.ac.jp, jun.kobayashi@akita-pu.ac.jp

ABSTRACT :

For multistory RC frame buildings, side columns or corner columns may encounter drastic varying axial load during strong motion. Substructure pseudo-dynamic tests of multistory RC frame (frame with soft first story and frame with weak-beam type) buildings were carried out. In the tests, two loading systems of RC specimens, which represent side columns of the first floor, were developed. The operator-splitting (OS) method was used as the numerical algorithm for analysis. Three pseudo-dynamic tests with different frame types and different shear reinforcement ratio specimens were executed successfully, and characteristic structural performances of side columns, which mainly depend on the building type, were elucidated.

KEYWORDS: RC column, varying axial load, substructure pseudo-dynamic test, frame with weak-beam type, dynamic response analysis

1. INTRODUCTION

It is recognized that especially for multistory RC frame buildings, the side columns encounter varying axial load during strong motions and also that the structure performance of columns subjected to varying axial force differs from that subjected to constant force. The authors have already developed a substructure pseudo-dynamic test method, which can add varying axial loads caused by random seismic motion to two RC column specimens, and by using this method, twelve stories RC frame building tests have been performed[1,2]. The characteristics of this method are that two RC column specimens can be loaded simultaneously and also that the inflection point of the columns can be changed by loading moment to rotate the top of the column. In this work, substructure pseudo-dynamic tests were performed for two kinds of RC frame (frame with soft first stories and frame with weak-beam type), and investigated the different behaviors of side columns such as axial force, restoring force and structural damage.

2. OUTLINE OF THE TEST

2.1. Building Models

The outlines of the frame models are shown in Fig.1. The two side columns of the first floor (shown by A and B in Fig.1) are the tested parts, which are replaced with two specimens. These model frames are a part of single frame of a building. Each frame model has 12 stories and two spans. The length of each span is 7,000mm and the inside height of each floor is 3,000mm. In this test, different types of building model, that is, a RC frame with weak-beam type [Fig.1(a)] and a RC frame with soft first stories [Fig.1(b)], were applied. Hereafter, the weak-beam frame is referred to as frame-I, and the frame with soft story as frame-II. The frame-I was designed on the basis of the ultimate strength concept[3]. For the frame-II, dimensions of columns and beams, and material properties were designed to be the same as those for the frame-I, however, shear walls of 200mm depth were added to second - twelfth floors, and the first story was designed so as to yield by bending at the top and the bottom of each column. The weight of each floor of each frame was 1,350kN, which was calculated by assuming that the weight of 1 m^2 floor was 1 ton.

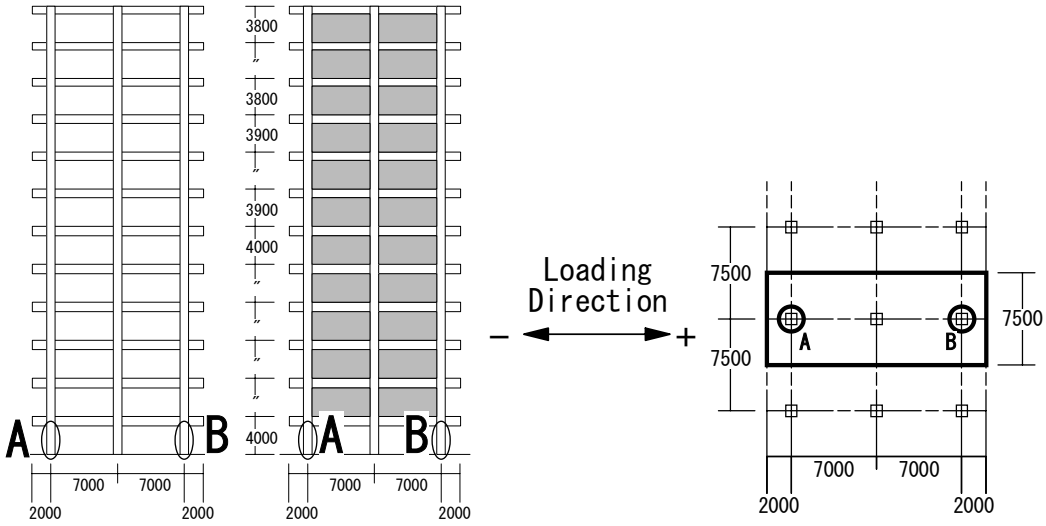

(a)Weak-beam frame (No.1) (b)Frame with soft story (No.2,No.3) (c)Plane of the frame [mm]

Figure 1 Outlines of model frames [mm]

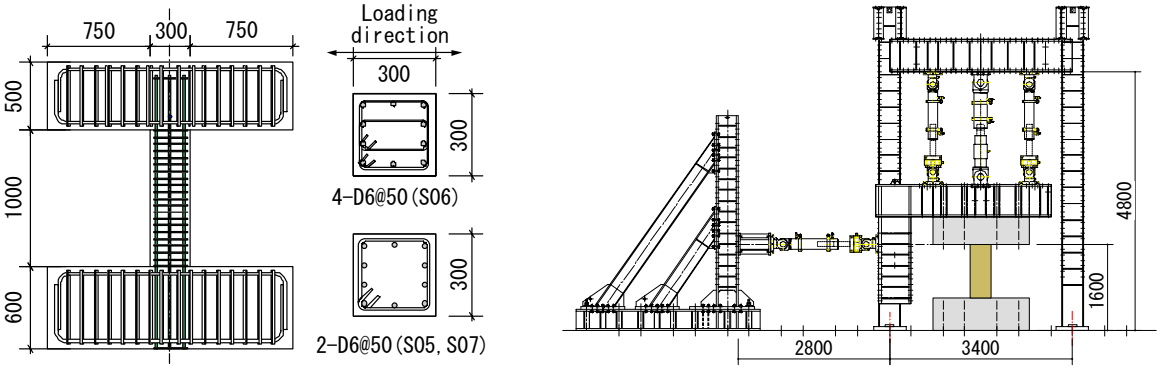

(a) Details of the column specimen (b) Loading system

Figure 2 Test setups

Table 1 Outlines of the specimen

Test No.	Frame type	Cross section	Height (mm)	Main bars (ratio)	Hoop (ratio)
1	Frame-I	300 x 300	1,000	10-D16 (2.2%)	2-D6@50 (0.42%)
2	Frame-II				4-D6@50 (0.84%)
3					2-D6@50 (0.42%)

The primary natural periods of the frame-I and frame-II are 1.20 s and 0.63 s, respectively, and the respective base shear coefficients are 0.30 and 0.33. In the tests, the fixed base condition was adopted. Therefore, the first floor columns are connected directly to the base.

2.2. Specimens of Tested Part

The outline of the specimen is shown in Fig.2(a) and Table 1. The dimension of the specimen was 300x300mm section and 1,000mm height, which was 1/3 scale of the frame model. As shown in Table 1, three different patterns of tests were executed. The test parameters were the frame model (No.1 for frame-I, No.2 and No.3 for frame-II) and the quantity of shear reinforcement. While the shear reinforcement pattern was the same in No.1 and

No.3 tests, the shear reinforcement in No.2 test was twice that in No.1 and No.3. In each test, two specimens were used as the side columns of the first floor. The yielding strengths of the longitudinal and transverse reinforcement were 377N/mm^2 and 350N/mm^2, respectively. The compressive strength of the concrete was 24.3N/mm^2 and the axial force ratio of the initial vertical load was 0.27.

2.3. System Setup of Substructure Pseudo-dynamic Test

The pseudo-dynamic test system used in this work is shown in Fig.3. The system consists of two sets of tested part, the analysis and main management part (PC for numerical analysis and main management), and the data acquisition part (PC for measurement). The main management part controls the total system during the tests. The main PC is connected to the computers for control (1) and (2), which control the tested parts, by LAN (TCP/IP) cables. The main PC is connected to the PC for measurement via a RS232C serial cable, through which the main PC sends command signals to each part, such as the target displacement and forces assigned for the tested parts, and data acquisition part after each loading step is completed.

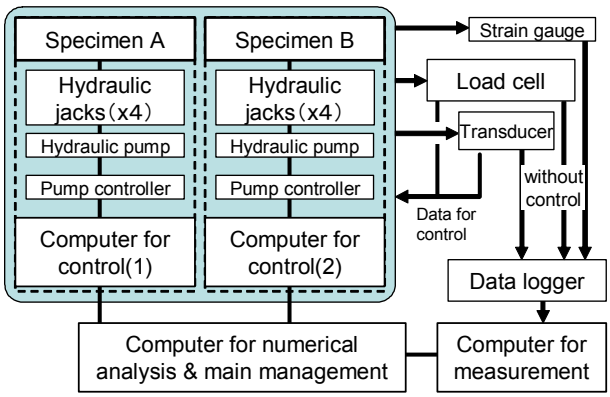

Figure 3 Outline of the substructure pseudo-dynamic test system

2.4. Test Setup

The test setup is shown in Fig.2(b). One of the characteristics of this work is to use two specimens for two side columns of the first floor as described in **2.1**. Therefore, two sets of test loading systems were prepared.

Here, each specimen must interact simultaneously with other beams, columns and wall as a part of the frame. Therefore, four static hydraulic jacks were installed to each specimen so that loading with three degrees of freedom (horizontal direction, vertical direction and rotational direction at the top of the specimen) could be performed. The middle jack in the vertical direction had a force capacity of 2MN and the force capacities of other two vertical jacks and one horizontal jack were 500kN. The controller of each jack can adopt either force- or displacement - control independently. Each controller was connected to the PC for control via RS232C serial cables, and each loading setup was controlled by the PC using programs developed in this study. In this setup, the jack in the horizontal direction was placed at the same height as the underside of the top stub of the specimen and used for horizontal seismic loading. The axial force, which includes varying axial force exerted by the vertical load, was controlled by the middle jack in the vertical direction. Two other jacks were used to control applied force in the rotational direction. Each degree of freedom was controlled as follows.

Horizontal direction: The horizontal displacement was measured by a displacement transducer, and the load of the load cell of the horizontal jack was fed back to the main PC.

Vertical direction: Since both the load and axial stiffness were remarkably larger than those for other degrees of freedom, not the displacement control but the force control was adopted. Here, the target displacement was preliminarily converted to the target axial force by the main PC and used for the force control. The axial force was the sum of loads measured by the load cells of the all vertical jacks.

Rotation at the top: The rotational angle was obtained from the difference between the displacements measured by the vertical displacement transducers situated at the both sides of the specimen and the horizontal distance between these two displacement transducers. Digital displacement transducers were used to measure displacements and rotational angles. The moment was calculated from the load measured by the load cells attached to the two vertical

jacks at the both sides and the horizontal distance between the two jacks, and this value was fed back to the main PC. Here, the total load of the two jacks was controlled to be constant. Before the start of experiments, the unbalance moment, which resulted from the L-shaped loading frame on the top of the specimen, was offset using the two vertical jacks at the both sides. Unlike analog displacement transducers based on the electric potential, the digital displacement transducer can measure the displacement with a resolution of 1/1000 mm. The difference between the target displacement and the current displacement was set at ±3/1000mm, and the loadings in the three directions were performed simultaneously. Two more jacks were added to maintain the horizontal deformation in the direction perpendicular to the loading direction at 0.

2.5. Algorithm of Substructure Pseudo-dynamic Test

The integration method using the operator-splitting (OS) method was applied in the tests. This method has been used in many substructure pseudo-dynamic experiments, and makes it possible to calculate earthquake response under the interaction between the specimen and the whole frame. The formulations of this method proposed by Nakashima et al.[4,5] are as follows:

$$Ma_{n+1} + Cv_{n+1} + K^I d_{n+1} + K^E_{n+1}\tilde{d}_{n+1} = P_{n+1} \quad (1)$$

$$\tilde{d}_{n+1} = d_n + \Delta t v_n + (\Delta t/2)^2 a_n \quad (2)$$

$$d_{n+1} = \tilde{d}_{n+1} + (\Delta t/2)^2 a_{n+1} \quad (3)$$

$$v_{n+1} = v_n + (\Delta t/2)(a_n + a_{n+1}) \quad (4)$$

Here, which K^I and K^E_{n+1} are the linear and non-linear stiffness matrices, M and C are the mass and viscous damping matrices, $\tilde{d}$ and d are the predictor and corrector displacement vectors, v and a are the velocity and acceleration vectors, and Δt is the integration time interval, respectively. The characteristic of this method is to divide the stiffness of the whole structure into a linear stiffness for the analysis part and a non-linear stiffness for the tested part (specimen). For the non-linear tested part, the explicit predictor-corrector method was used. By associating the non-linear stiffness with the linear stiffness integration method, the Newmark-β method could be applied to the whole part. When the linear stiffness is much larger than the non-linear stiffness, the integration method is unconditionally stable. In this work, Eqn. (1) - (4) were transformed into the incremental equations, that is, equations for obtaining $\Delta\tilde{d}$, Δd, Δv and Δa. It was confirmed that even when the incremental form equations were applied, the condition where the linear stiffness is always larger than the non-linear tangent stiffness and the integration method gives stable solutions is the same as that when the original equations were used.

The procedure of the substructure pseudo-dynamic experiments are as follows:

(1) By using the integration method (OS method), the target predictor displacement at the next step is calculated. The main PC is used in this calculation.

(2) The main PC sends the target displacements (horizontal displacement and rotational angle at the top of column) to the PCs for control (1) and (2), which control the loading systems.

(3) Until the current displacement reaches the target value, the specimens are loaded by the four jacks under the control of PCs for control.

(4) The restoring forces (horizontal load and the moment at the top of column) are measured when the displacements reach the target values by the load cells attached to the jacks, and the values are fed back to the main PC.

(5) After the restoring forces are fed back to the main PC, it sends a command to the data acquisition PC for asking acquisition of experimental data.

(6) After the data acquisition is completed, the procedure (1) is performed using the data on the restoring force and input acceleration.

In the tests, the integration time was set at 0.01 s. The Rayleigh damping was applied and the viscosity damping property was set at 5%. A ground motion recorded at the Tohoku University in the 1978 Off Miyagi Prefecture earthquake (EW direction) was chosen as the input ground motion. The test was divided into 4 levels (Run 1 to

Run 4), from the weak elastic response level to the strong plastic response level. The maximum acceleration of input ground motion for each level is shown in Table 2. The input level of the maximum acceleration was adjusted so that the maximum horizontal displacement of the first floor for the frame-I was the same as that for the frame-II at each run. Prior to experiments, dynamic analyses of frame-I and frame-II were performed to determine the maximum acceleration. Here, the numerical model was applied to the whole frame.

Table 2 Input levels of each frame

Input Levels	Frame-I	Frame-II	Target story drift angle [rad]
RUN1	200gal	140gal	1/400
RUN2	600gal	220gal	1/200
RUN3	900gal	370gal	1/100
RUN4	1,500gal	640gal	1/40

2.6. Analytical Models of the Frame

The columns and beams in the analytical part and the shear wall for the frame-II were modeled as the line elements. Inelastic rotational springs were added to the both ends of each beam, and multi-springs (MS) were added to both ends of each column. The shear wall combined with the middle column and the columns on the both sides were modeled as a single line element, and similarly to the column model, five multi-springs were set on the both ends. The outlines of the respective models are shown in Fig.4. The tri-linear hysteretic model was used for the inelastic rotational springs.

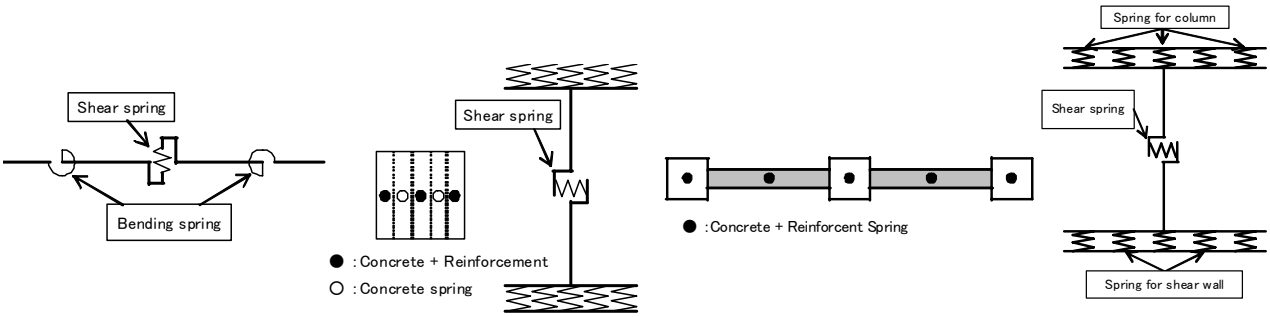

(a) Beam model (b) MS model for column (c) MS model for shear wall

Figure 4 Applied analytical model

3. RESULTS OF THE TEST

3.1.Outlines of test results

Fig. 5 shows the time history response of the horizontal drift of the specimen of the first floor observed in Run 3 and Run 4. In the case of No. 1 test for frame-I, experiments could be successfully performed by the end of Run.4 without shear failure of the specimen. However, in the case of No. 2 and No.3 tests for frame-II, experiments ended at different points during Run 4 and during Run 3, respectively, due to the loss of axial load capacity. No.2 and No.3 tests showed almost the same time history response of the horizontal drift until the specimen of No.3 lost axial load capacity.

Target and measured values of the horizontal displacement, rotational angle and axial force for Run 3 of No.1 test (Specimen A) are shown in Fig. 6(a). These two values are almost same, indicating that the loading systems could give the same displacement to both the specimen and the connecting elements of the frame. Differences between these target values and measured values are shown in Fig. 6(b). The red lines in the figure show the allowable ranges of the differences (±0.003mm for horizontal displacement, $\pm 6\times10^{-6}$ rad for rotational angle and ±5kN for axial load). At almost all steps of the tests, the differences were within the allowable ranges.

Damage patterns observed after the tests are shown in Fig.7. In No.2 and No.3 tests, shear cracks and bending cracks were observed in the specimen during Run 2, and longitudinal cracks were observed on the top of the specimen. During Run 3, the cracks observed in Run 2 developed and when the axial force was larger, peeling of cover concrete was observed both on the top and bottom of the specimen. On the other hand, in No.1 test, shear

cracks and bending cracks formed during Run 2 similarly to other tests, and the cracks formed mainly on the bottom. During Run 4, with increasing the horizontal displacement, cracks gradually developed. However, the crack and peeling damage in No.1 test was less than that in No.2 and No.3 tests. In No.2 and No.3 tests, the main reinforcement of the specimen yielded when the axial force was on the pull range during Run 2, and in No.1 test it yielded during Run 3. Almost the same maximum response horizontal displacement of the specimen was observed during Run 1 and Run 2 in all tests. However, during Run 3, it became larger than the expected values in No.2 and No.3 tests with frame-II, and it became almost the same value as that observed during Run 4 in No.1 test (frame-I). This is because the restoring forces of the specimens were deteriorated due to developed crack damages after flexural yielding in No.2 and No.3 tests. Moreover, unlike frame-I, in the case of frame-II, the soft first story suffered almost all damages of the frame, and decreased restoring force increased the maximum response.

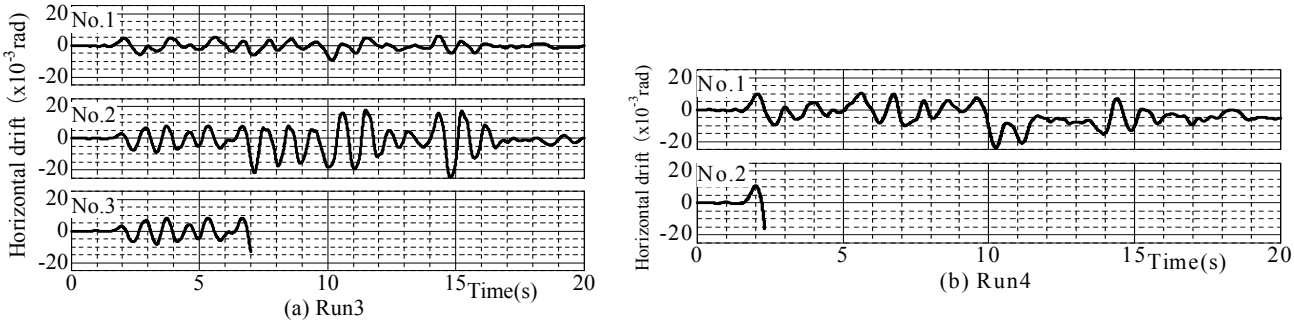

Figure 5 Time history of horizontal drift at first floor

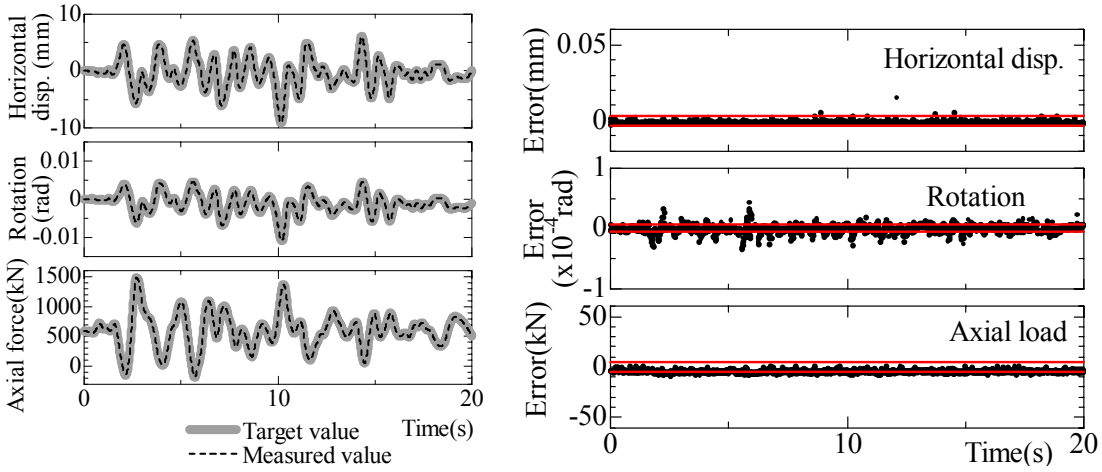

(a) Target value and measured value (b) Difference

Figure 6 Comparisons between target and measured values (Run 3, Specimen A)

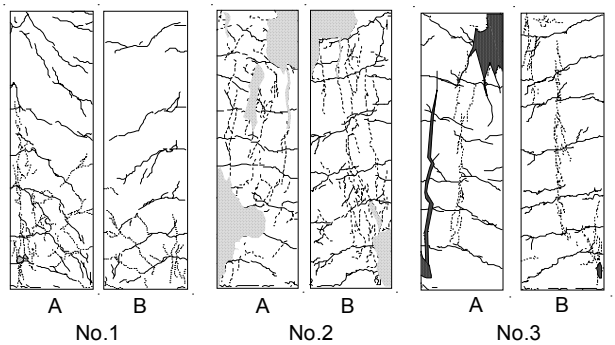

Figure 7 Crack patterns of specimen after test

3.2.Relationship between horizontal load and horizontal drift

Fig.8(a) shows the relationship between the horizontal load and horizontal drift observed with specimen A. The specimens A and B represent the left and right columns of the frame, respectively. The axial force of the specimen A decreases as the specimen moves to the positive (right) direction, and it increases as the specimen moves to the left direction. Therefore, the horizontal load became large in the left region of Fig.8(a) and became small in the right region for specimen A. The widths of the hysteresis loops observed in No.2 test were small compared to those observed in No.1 test. The maximum load observed in No.1 test was small in the high axial force region compared to those of No.2 and No.3 tests. In all tests, the maximum response drifts observed during Run 2 were almost the same (1/200 rad), however, the maximum horizontal loads in No. 2 and No.3 were about twice that in No.1. In addition, the maximum response drift during Run 4 in No.1 test was approximately equal to that during Run3 in No.2 test (1/40 rad), however, the maximum horizontal load in No.2 was about 1.5 times that in No.1.

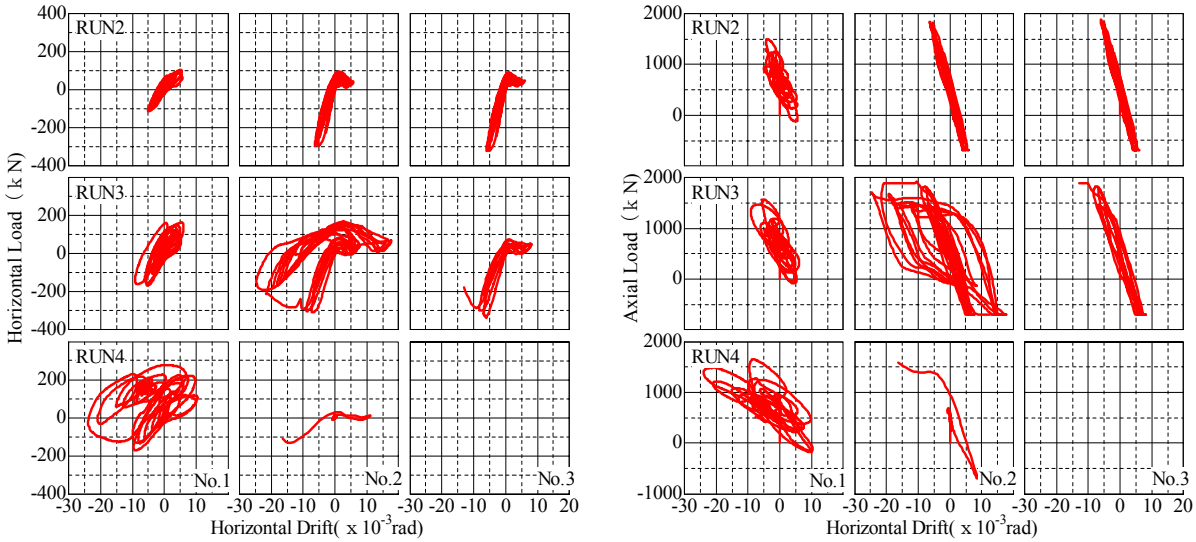

(a) Horizontal load - horizontal drift relationships (b) Axial force - horizontal drift relationships

Figure 8 Results of specimen A

3.3.Relationship between axial load and horizontal drift

Fig.8(b) shows the relationship between the axial load and horizontal drift. In No.1 test, as the position of the peak of the axial force does not always agree with that of horizontal drift probably due to the higher mode effect, linear relations were not observed. On the contrary, in No.2 and No.3 tests, linear relations were observed during Run 2. For frame-II, the higher mode effect was suppressed due to the soft first story and therefore, the positions of the peaks agreed. In No.2 test, the horizontal drift exceeded 1/100 rad during Run 3, and the hysteresis loop changed from a linear shape to a spindle-shaped curve.

3.4.Inflection Points of the Specimen

Fig.9 shows the variation in the height of inflection point during Run 2 of all tests (Specimen A). Here, the ordinate is the inflection point ratio, defined by the ratio of the height to the specimen height. The inflection point ratio always varied and did not become constant probably due to the response of the frame and the variations in the axial force. While the inflection point ratio ranged from 0.75 to 1.00 when the horizontal load was large in No.1 test, it was around 0.5 in No.2 and No.3 tests.

For frame-I (No.1 test), the inflection point moved to the upper part of the column due to a larger rotation angle of the column top. On the other hand, for frame-II, the rotation of the column top was constrained due to the shear wall located on the floors above the second floor. Therefore, the inflection point remained in the middle part of the column. The shear span ratio increased linearly with the inflection point ratio. As a result, the horizontal shear force decreased and the damage of the column top decreased. This may be the reason why the damage of the specimen in No.1 test was smaller than those in No.2 and No.3 tests, and the maximum horizontal load in No.1 test was much smaller than those in No.2 and No.3 tests.

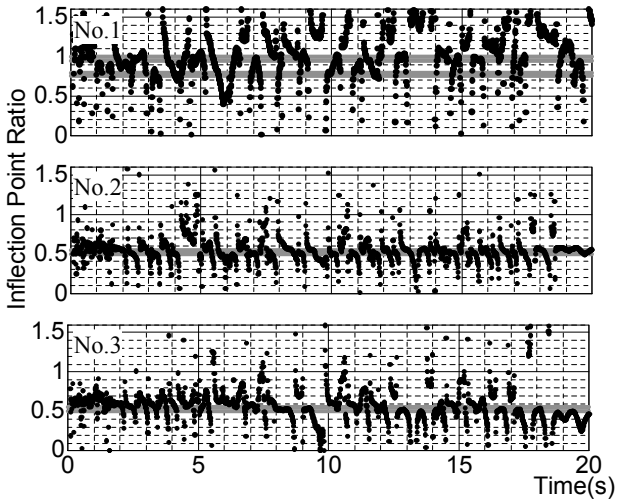

Figure 9 Inflection point of each step(Run3, Specimen A)

4. CONCLUSIONS

A series of substructure pseudo-dynamic tests was successfully performed to investigate the dynamic behavior of the side columns of the first floor of two kinds of multistory RC frame (RC frame with soft first stories and RC frame with weak-beam type) buildings. The side columns were subjected to varying axial loads.
It was found that the axial force - horizontal displacement relation and the inflection point of the side column differ depending on the frame. As a result, even for the same horizontal displacement, the side columns in the RC frame with soft first story were more damaged than those in the frame with weak-beam type. It was also found that for the same frame, the seismic response was almost the same independently of the quantity of transverse reinforcement until the specimen collapsed.

REFERENCES

[1]Teramoto, N. Nishida, T. and Kobayashi, J. (2006). A loading test of two side-columns of a RC frame with use of substructure pseudo-dynamic test method (In Japanese). *Proceedings of the Japan Concrete Institute* **28:2**, 217-222.

[2]Nishida, T., Teramoto, N. and Kobayashi, J. (2007). Effect of Varying Axial Force on seismic Behavior of 1st Floor Side Columns of a 12-Story RC Frame (In Japanese). *Proceedings of the Japan Concrete Institute* **29:3**, 967-972.

[3]Architectural Institute of Japan. (1990). Design Guidelines for Earthquake Resistant reinforced concrete buildings Based on Ultimate Strength concept (In Japanese). Architectural Institute of Japan, Japan.

[4]Nakashima, M., Kaminosono, T., Ishida, M. and Ando, K. (1990). Integration techniques for substructure pseudo-dynamic test. *4th US National Conference on Earthquake Engineering* **Vol.2**, 515-524.

[5]Pan, P., Nakashima, M. and Tomofuji, H. (2005). Online test using displacement-force mixed control. *Earthquake engineering and Structural Dynamics* **34:8**, 869-888.